

MATLAB/Simulink Framework for Modeling Complex Coolant Flow Configurations of Advanced Automotive Thermal Management Systems

2016-01-0230

Published 04/05/2016

Gene Titov, Jason Lustbader, and Daniel Leighton

National Renewable Energy Laboratory

Tibor Kiss

Thermal Sciences Consulting

CITATION: Titov, G., Lustbader, J., Leighton, D., and Kiss, T., "MATLAB/Simulink Framework for Modeling Complex Coolant Flow Configurations of Advanced Automotive Thermal Management Systems," SAE Technical Paper 2016-01-0230, 2016, doi:10.4271/2016-01-0230.

Copyright © 2016 SAE International

Abstract

The National Renewable Energy Laboratory's (NREL's) CoolSim MATLAB/Simulink modeling framework was expanded by including a newly developed coolant loop solution method aimed at reducing the simulation effort for complex thermal management systems. The new approach does not require the user to identify specific coolant loops and their flow. The user only needs to connect the fluid network elements in a manner consistent with the desired schematic. Using the new solution method, a model of NREL's advanced combined coolant loop system for electric vehicles was created that reflected the test system architecture. This system was built using components provided by MAHLE Inc. and included both air conditioning and heat pump modes. Validation with test bench data and verification with the previous solution method were performed for 10 operating points spanning a range of ambient temperatures between -2°C and 43°C. The largest root mean square difference between data and simulation results for pressure, temperature, energy and mass flow rate was less than 7%.

Introduction

When operating, the air conditioning (A/C) system is the largest auxiliary energy consumer in a conventional vehicle. A/C loads account for more than 5% of the fuel used annually by light-duty vehicles in the United States [1]. Climate control loads can have an even larger impact on hybrid electric vehicle (EV), plug-in hybrid EV, and all-electric vehicle performance. Hybrid EVs show a 22% lower fuel economy with the A/C on [2]. For all-electric vehicles, the effect of the climate control system usage is even more severe. Due to a shortage of waste heat, heating of the passenger cabin in EVs has to rely on battery energy. Cooling the cabin can also take a significant portion of energy available in the battery, significantly reducing vehicle efficiency and range. Mitsubishi reports that the range of the i-MiEV can be reduced by as much as 68% with heating and 46% with cooling of the cabin on Japan's 10-15 cycle [3]. The Advanced

Powertrain Research Facility at Argonne National Laboratory has reported 59.3% and 53.7% reductions in range due to maximum heating and maximum cooling, respectively, for the Ford Focus EV operating on the Urban Dynamometer Driving Schedule cycle [4]. In addition to these climate control impacts, electric-drive vehicles may have additional cooling requirements for the electric traction drive system components, including batteries, power electronics, and electric machines.

To solve these challenges, alternative heating methods and more efficient cooling systems are needed for EVs. These methods often involve running the A/C system in heat pump mode to reduce the heating power requirements of the cabin. In some advanced concepts, the traditional liquid coolant-based thermal management is supplemented with refrigerant-based cooling systems, which can make the thermal management system as a whole significantly more complex. When developing a thermal management system for an internal combustion engine vehicle, it has traditionally been sufficient to simulate the A/C system and the liquid coolant-based cooling system separately. For advanced vehicles, especially for hybrid and all-electric vehicles, the benefits of interconnectedness of the thermal management and A/C systems outweigh the associated complexity. This, in turn, results in a requirement for more integrated simulation approaches.

The more complex thermal management systems of advanced vehicles typically allow for various modes of operation that can be selected based on driving and ambient conditions. Investigating a number of system alternatives and determining the best ranges for various operating modes with experimental methods can be very time consuming. A good system simulation tool can greatly reduce the time and expense of developing these complex systems. Such tools should also be able to efficiently co-simulate with vehicle simulation programs and should be applicable for evaluating various control algorithms. The

MATLAB/Simulink simulation environment, popular in the automotive industry, is well suited for development of such models and meets the requirements of dynamic modeling of complex systems.

Background

To meet the needs of advanced vehicle thermal system simulations, the U.S. Department of Energy's National Renewable Energy Laboratory (NREL) is building an integrated single- and two-phase thermal system modeling framework, CoolSim, in Simulink. This integrated approach allows for rapid system analysis and design in a flexible and open modeling environment. Simulink is a common engineering platform that allows for co-simulation with vehicle modeling software Autonomie [5]. NREL previously developed an A/C system simulation modeling framework in MATLAB/ Simulink and validated its results against test bench data. To match the wide range of A/C modeling needs, NREL developed models with three different levels of detail: the Fully-Detailed, Quasi-Transient, and Mapped-Component models.

The three models involve different levels of trade-offs between speed and accuracy to meet a wide range of modeling needs. The Fully-Detailed model captures the system transient behavior accurately but runs at 0.1 of real-time speed [6]. The Quasi-Transient and Mapped-Component models are progressively more simplified while trying to maintain accuracy and run at real-time speed and faster than 10 times real-time speed, respectively [7]. The goal of these newer model versions was to provide faster simulation tools for less detailed, vehicle-focused drive-cycle-based evaluations of A/C systems. For steady-state conditions, the Quasi-Transient model provides essentially the same accuracy as the Fully-Detailed model. The Mapped-Component model does lose some accuracy in steady-state conditions. For the SC03 drive cycle, the averaged results of power and heat exchange rates obtained with the Quasi-Transient model are within 3% of the results of the Fully-Detailed model. The Mapped-Component model results are within 15% of the results of the Fully-Detailed model. Short transients, such as those occurring during compressor cycling, produce the most deviation from the Fully-Detailed model for both simplified models. Conversion from the Quasi-Transient A/C system model approach to the other two models is relatively simple within the CoolSim framework. This allows a new system model to be developed with the Quasi-Transient version before the results are refined using the slower Fully-Detailed version or accelerated using the faster Mapped-Component model version.

As outlined in the Background section, there is a need for coupled thermal system simulations due to interconnectedness of the refrigerant and liquid coolant circuits used in advanced thermal management systems, especially the ones developed for EVs. To address this need, NREL's refrigerant circuit simulation model was extended with a liquid-coolant circuit simulation capability. The originally implemented coolant Fluid Network solution method [8] was selected for its speed and algorithmic simplicity. This approach works well for relatively simple systems that do not involve features such as changes in fluid flow direction, a large number of operating modes, etc. The complexity and flexibility of next generation integrated systems, however, put a higher burden on the user for setting up the models using the originally developed Fluid Network

approach. Certain system configurations with changing flow directions based on mode and operating conditions were also found to be challenging to simulate. To improve modeling of these more complex thermal systems, a more general method that considers the coolant as a compressible medium with an artificially small bulk modulus was developed. This approach is similar to that used for two-phase flow of refrigerant in the Quasi-Transient method.

While this approach comes at a higher computational cost, the flexibility and ease of model development make it a preferable alternative for complex fluid networks. Furthermore, it was determined that the bulk of computational effort is typically spent on the refrigerant circuit, making additional computational expenses relatively small. An additional benefit for developers comes from the fact that the solution methods for both single- and two-phase flows become similar. As a result, the effort spent on developing models in the CoolSim framework for specific systems is reduced.

A model built with this updated version of CoolSim was developed for NREL's combined fluid loop (CFL) thermal management test bench in both active cooling and heating modes. Comparisons of simulated results with measured data validate the new coolant loop solution approach. Additional verification was obtained by comparisons with results produced by the Fluid Network solution method.

A New Approach to Coolant Loop Modeling

The new single phase solution method integrates the "Quasi-Transient" modeling method for the refrigerant circuit with a similar approach for coolant loops. The details of the two-phase refrigerant loop solution method are discussed in [7]. This paper focuses on details of the single-phase coolant loop modeling. The original Fluid Network approach for solving coolant loops in CoolSim relies on a theory similar to Kirchoff's law for electric circuits. This approach is efficient and will continue be of use for simpler systems; however, the approach proved to be complicated for quick development of more sophisticated models with many modes of operation. [Figure 1](#) shows the model interface in Simulink for the original solution approach and [Figure 2](#) shows the new approach interface. Although the new interface looks more involved, the time needed to build and test the new model was notably less due to elimination of a coolant loop specification step of the original approach. An important advantage of the new approach is its ability to simulate complicated multi-mode fluid networks with changing flow directions in straightforward manner.

Similar to the Quasi-Transient refrigerant circuit approach, coolant loops in the new method are represented by zero-dimensional (0-D) volume simulation blocks connected with simulation blocks for one-dimensional (1-D) pipes, valves, or orifices. In general, any system component that can provide a flow rate due to a pressure differential can be connected to the 0-D volume blocks. For the coolant loop network topology, these 0-D volume blocks are referred to as junctions, as opposed to actual fluid reservoirs such as accumulators, headers, compressor suction/exit volumes, etc., in case of refrigerant circuits. These coolant junction simulation blocks can still be used to model large volumes of coolant if needed.

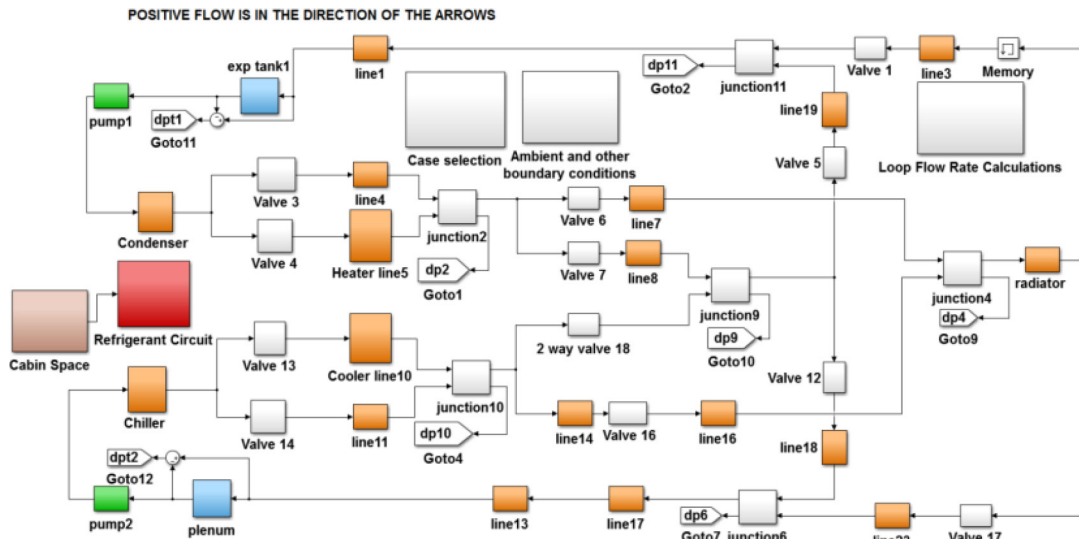


Figure 1. Original approach. NREL combined loop model, Simulink top-level view

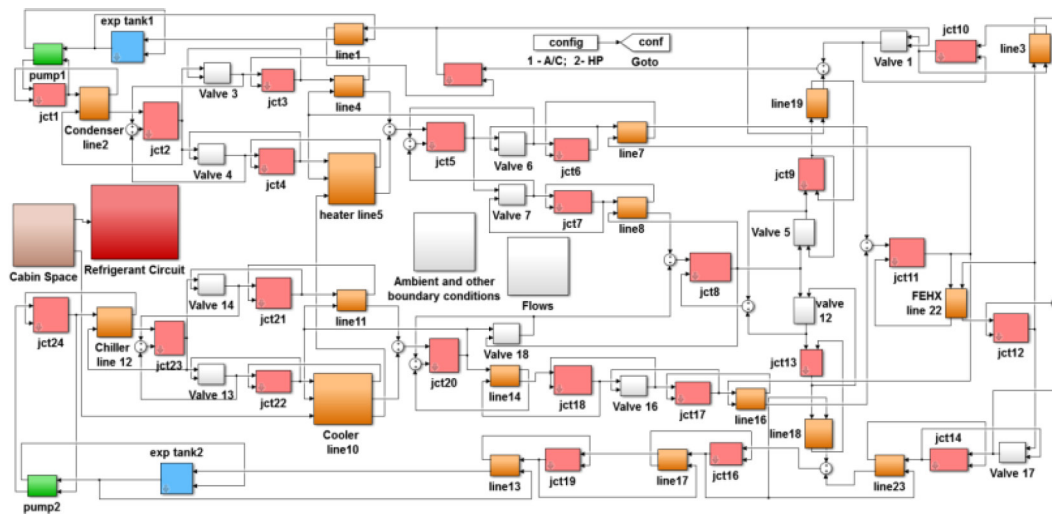


Figure 2. New approach. Combined loop model, new approach Simulink

The strategy of this new Quasi-Transient single-phase numerical method is to approach a steady-state solution that corresponds to the boundary conditions prevailing at each of the time steps. In this way, the model approximates a solution that would be obtained with a hypothetical quasi-steady-state model that at every time step computes steady-state conditions for the entire system. In 0-D junctions, a compromise is made between the accuracy of the implemented conservation equations and computational speed. This is achieved by introducing and adjusting an artificial bulk modulus, which ensures that all volumes in the model have similar low numerical stiffness so that the high stiffness of liquid is avoided. This allows for significantly larger computational time steps while maintaining numerical stability and accuracy, resulting in faster simulations.

The 1-D pipe block assumes a constant coolant mass flow rate along its length. The flow rate then becomes a simulation state variable. At each time step, the coolant pressure differential across each line is compared to pressure differences between the junctions (0-D volume blocks) attached to them. A numerical method is applied to continuously adjust the coolant mass flow rate in each of the lines. The goal of this method is to match the pressure drop of the line to the

pressure drop between the junctions that the line connects. The coolant mass flow rate, therefore, responds with a delay but it approaches the solution that would develop under the steady-state conditions.

The downside of this approach is that the total coolant mass in the system is fluctuating slightly and the energy balance is not strictly enforced. The implications include lost accuracy for modeling of fast transients that occur on the order of seconds, such as pump cycling. For steady-state conditions, however, the conservation of mass and energy for each junction and each of the 1-D pipes in the model is ensured. A typical thermal management network is a slowly drifting “quasi-steady” system, especially in cases with constant-RPM electric pumps. In such cases, a true conservation of mass and energy will be closely approximated by this method at all times.

Junction Modeling

For junctions, a mathematical concept of “artificial mass” of coolant is introduced and the conservation equations are written for this artificial mass. This allows for adjustment of system “stiffness.” Mass and enthalpy flows into and out of a junction are obtained from adjacent blocks. The heat transfer rate across the solid boundary of a junction is obtained separately. The time derivative for the artificial

mass in a junction volume is the difference between the sum of incoming and the sum of outgoing mass flow rates as is formulated by the following equation:

$$\frac{dm_a}{dt} = \sum_i \dot{m}_{in,i} - \sum_j \dot{m}_{out,j} \quad (1)$$

where m_a is the artificial mass, t is time, and $\dot{m}_{in,i}$ and $\dot{m}_{out,j}$ are incoming and outgoing mass flow rates, respectively. Conservation of energy is treated in a similar manner in a form of a control volume equation. The size of the volume is constant, which implies that there is no work done by solid boundaries. The resulting time derivative of the total energy in a junction volume is the sum of incoming enthalpy flow rates minus the sum of outgoing enthalpy flow rates plus heat addition:

$$\frac{dU}{dt} = \sum_i \dot{H}_{in,i} - \sum_j \dot{H}_{out,j} + \dot{Q} \quad (2)$$

where U is the internal energy, \dot{H}_{in} and \dot{H}_{out} are the enthalpy flow rates in and out of the volume, respectively, and \dot{Q} is the heat transfer rate into the volume through its boundaries.

Naturally, m_a and U are simulation state variables. By integration, Eqs. (1) and (2) produce the artificial mass and total energy in a junction, making these values available before values of all the other variables are computed as time is advanced by a step.

The artificial coolant mass is introduced to allow changing how pressure and density are related through the coolant material property equations. This approach assumes a uniform coolant bulk modulus valid for all conditions, making pressure a function of the artificial density only. The bulk modulus is also proportional to the size of the volume. This ensures that all junction volumes in the model have adjustable and identical ‘‘stiffness,’’ meaning similar coolant flow rates will result in similar pressure changes regardless of the size of the volume. The result is a higher allowed simulation time step and therefore a much faster model execution.

Accordingly, the pressure in a junction is:

$$p = B \cdot \left(\frac{m_a}{V} - \rho_{ref} \right) \quad (3)$$

where B is the bulk modulus measured in Pa, V is the size of the volume, and ρ_{ref} is a reference density. Note that while volume V is varying from junction to junction in the system, B/V for each of junction remains the same. B/V and the volume are input parameters from which B is calculated. The lower the value of B/V , the ‘‘softer’’ the system will be. By dividing the total enthalpy by the artificial mass, the specific enthalpy in the volume can be obtained as:

$$h = \frac{U + pV}{m_a} \quad (4)$$

Temperature is calculated from the specific enthalpy, using the generic enthalpy-temperature relationship for a specific coolant.

Equations (1) and (2) become accurate for conservation of mass and energy when applied to steady-state conditions. If the sum of incoming mass flow rates is greater than the sum of outgoing mass flow rates, the artificial mass will increase, and therefore the pressure in the volume will increase. Such a pressure rise will tend to reduce the incoming mass flow rates and will increase the outgoing mass flow rates. As a result, the system will be driven to a steady-state solution. A similar statement can be made for enthalpy, provided the mass flow rates in and out have already reached a steady state; therefore, Eqs. (1) and (2) approach the rigorous mass and energy conservation equations in steady-state conditions, and they will tend to drive the system towards a correct steady-state solution from any transient state.

1-D Pipe modeling

For the 1-D pipe model, the governing equations are also developed with the goal of approximating quasi-steady solutions. The approach assumes a constant coolant mass flow rate along the length of a pipe at any time. The flow rate is, however, allowed to vary in time. A finite volume formulation is used to determine the lengthwise distribution of flow parameters. With the coolant mass flow rate fixed along the length of the pipe, the finite volume equations can be applied with a marching scheme in the direction of the flow. For each finite volume (or segment) and at each time step, the flow variables at the outlet boundary of the segment can be calculated from the flow variables at the inlet to that segment and the wall temperature of the segment. Assuming that the magnitude and direction of the coolant flow are known, it can be considered that the inlet boundary conditions of the first segment are those prevailing in the junction attached at the upstream side of the pipe block. Starting with this condition, the pressure at the exit boundary of the first segment, p_{out} , is calculated using the Darcy-Weisbach equation (Eq. 5.8.7 in [9]).

$$p_{out} = p_{in} - 1/2 f \frac{L}{D_h} \rho_{in} v_{in}^2 \quad (5)$$

where P_{in} , ρ_{in} , and V_{in} are the pressure, density, and velocity at the inlet boundary of the segment; L is the length of the segment; D_h is the hydraulic diameter; V_{in} is the constant mass flow rate, \dot{m} , divided by the inlet boundary density, ρ_{in} and by the pipe cross sectional area. The wall friction coefficient, f is obtained from the Hagen-Poiseuille equation (Eq. 5.10.12 in [9]) for laminar flows and from a modified version of the Colebrook equation (Eq. 5.10.13 in [9]) for turbulent flows. Next, the local heat transfer coefficient is calculated with the Dittus-Boelter correlation [10] and the effectiveness-number-of-transfer-units (E-NTU) method [10] is applied to obtain the coolant exit temperature assuming that the pipe wall temperature is uniform. This approach ensures that the coolant exit temperature from the segment does not overshoot the wall temperature:

$$T_{out} = T_{in} - (T_{in} - T_w) \cdot \left(1 - \exp \frac{\alpha A}{\dot{m} C_p} \right) \quad (6)$$

where T_{in} is temperature at the inlet boundary, T_w is the segment wall temperature, A is the heat transfer area (segment length times inner channel perimeter), α is the heat transfer coefficient, and C_p is the constant pressure specific heat. Then, the heat transfer rate from the coolant to the wall can be calculated as follows:

$$\dot{Q} = C_p \cdot \dot{m} \cdot (T_{in} - T_{out}) \quad (7)$$

Once the heat transfer rate is computed with Eq. (7), the specific enthalpy on the outlet boundary can also be calculated with:

$$h_{out} = \frac{\dot{H}_{in} - \dot{Q}}{\dot{m}} \quad (8)$$

where \dot{H}_{in} is the enthalpy flow rate through the inlet boundary of the segment. With h_{out} and p_{out} obtained, all the other coolant properties can be calculated at the outlet boundary of the first segment. The procedure can be repeated for each subsequent segment of the line with outlet conditions at a previous segment serving as the inlet conditions for the subsequent one. This constitutes a ‘‘marching’’ scheme that starts at the upstream boundary of a pipe and proceeds until the downstream boundary is reached. The pressure obtained at the outlet of the pipe can now be compared to the pressure inside the junction connected to the pipe at its downstream boundary. Ideally, these two pressures would match, which would mean that the coolant mass flow rate used in the calculations was accurate; however, these pressures typically differ. One approach to resolve the difference is to iterate the coolant mass flow rate until the pressures match, which was found to be computationally expensive. A faster alternative approach was adopted in which only one iteration of the marching has to be completed per pipe for each time step. Instead of fully converging the system to an intermediate steady state, the pipe flow solution is advanced one iteration step toward the steady state. After a step is completed, the outlet pressure is compared to that of the junction downstream to calculate a rate of change for the coolant mass flow in the pipe. This rate is used to determine the mass flow rate for the next time step by the integrator. Therefore, the coolant mass flow rate becomes a simulation state variable, and it will be available at the beginning of each time step. The equation applied to calculate the derivative of the mass flow rate is as follows:

$$\frac{d\dot{m}}{dt} = C \cdot \frac{p_{d,calc} - p_d}{p_u - p_d} \cdot \dot{m}, \quad (9)$$

where \dot{m} is the coolant mass flow rate, p_u and p_d are the pressures in the upstream and downstream junction blocks respectively, $p_{d,calc}$ is the 1-D pipe downstream boundary pressure calculated at the current time step, and C is an input parameter that adjusts the rate of the numerical ‘‘pull’’ towards the steady-state solution at the given intermediate boundary conditions.

The air side heat transfer calculations are identical to those used in the quasi-transient model of the refrigerant system. To compute the heat flux, velocity, pressure and temperature of the air flow, as well as the average wall temperature, of each of the pipe segments are used.

The Chang correlation [11] is used for obtaining the heat transfer coefficient. The effect of fin efficiency is accounted for and the details of the calculations can be found in [6].

For calculations of both the internal (coolant-to-wall) and external (air-to-wall) heat transfer rates, an average wall temperature T_w in each of the pipe segments is needed. In fact, it is the wall temperature through which the internal and external flow calculations are coupled. The temperatures of the wall segments are simulation state variables; thus, their time derivatives are known at each simulation time instance. As the integrator advances from a particular time point to the next one (time increases by a time step) these wall temperatures will also be obtained for the new point in time. With the segment wall temperatures known, the internal and external heat transfer rates can now be calculated using Eqs. 6 and 7 and by following the procedure described in Ref 6. Finally, the time derivative of the average temperature of a wall segment is calculated so that the integrator may advance further in time. The time derivative of the wall temperature is obtained from the conservation of energy principle, which states that the net heat flux into the wall segment is the amount of energy stored in the wall segment:

$$\dot{Q}_{aw} - \dot{Q}_{cw} - \frac{d\dot{Q}_x}{dx} \cdot \Delta x = C_{pw} \cdot \Delta m_w \cdot \frac{dT_w}{dt} \quad (10)$$

where \dot{Q}_{aw} is the heat transfer rate from air to the wall, \dot{Q}_{cw} is the heat transfer rate from the wall to the coolant, \dot{Q}_x is the heat transfer rate in the pipe wall along the refrigerant flow direction, C_{pw} is the wall material specific heat, and Δm_w is the mass of the wall segment. The $\frac{d\dot{Q}_x}{dx} \cdot \Delta x$ term represents the imbalance in conductive heat flow rates from the neighboring wall segments. The time derivative dT_w/dt can now be calculated from Eq. 10 and used by the integrator to compute the wall temperature at the next point in time.

For increased simulation speeds, a variant of the method can be used that utilizes lookup tables for components represented by junctions and 1-D pipe models, a typical example being a heat exchanger. In such a method, the coolant mass flow rates are obtained from 1-D lookup tables relating mass flow rates to pressure differences across components. For heat exchange rates, lookup tables using coolant mass flow rates, coolant inlet temperatures, air mass flow rates, and air inlet temperatures as parameters can be used. To generate such lookup tables, separate models are typically created using junction and 1-D line models. These models can be simulated over the entire range of desired values of the above mentioned parameters to produce the lookup tables suitable for faster simulations.

Results

Validation of the New Coolant Modeling Approach

NREL’s CFL electric-drive vehicle thermal management system test bench [12], shown in Figure 3, was selected for validation and demonstration of the new coolant loop solution method. The complete system schematic is shown in Figure 4.



Figure 3. NREL's combined fluid loop test bench thermal management system apparatus

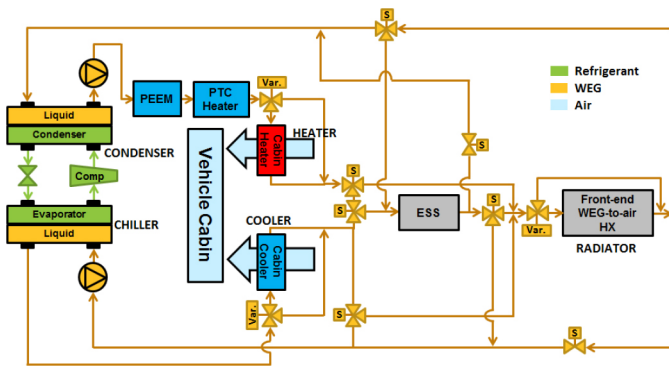


Figure 4. Schematic of NREL's CFL electric-drive vehicle thermal management system

Two modes of operation were selected for validation of the new coolant solution method that are of primary interest in connection with emerging thermal management systems of EVs: active cooling and heating that utilizes heat pumping from the outside environment using a vapor compression cycle. NREL's test bench allows for testing a wide range of advanced A/C, heat pump, and cooling loop configurations [10]. In this system, a refrigerant circuit operating the vapor compression cycle is used as both an A/C unit (providing cooling) and as a heat pump (providing heating). The refrigerant loop exchanges heat with the liquid coolant in the chiller and in the condenser. The liquid coolant is used to provide cooling and heating to the cabin.

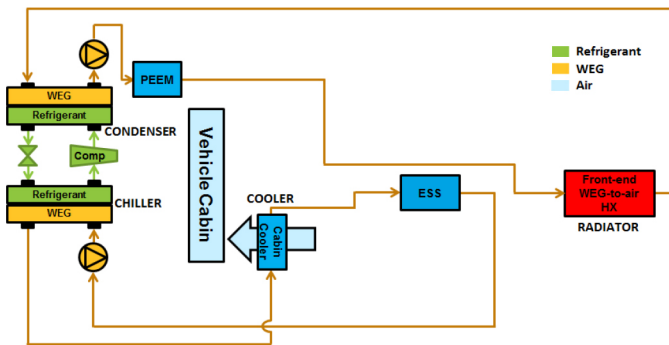


Figure 5. Active cooling mode

The schematics of the two modes selected for validation are presented in Figures 5 and 6. Figure 5 shows an active cooling mode in which the cabin is cooled by a liquid coolant that then exchanges heat with the refrigerant via a liquid-to-refrigerant chiller. The heat is

then released to a “hot” loop coolant via a liquid-to-coolant condenser and transferred to the ambient air through a coolant-to-air front-end heat exchanger (radiator).

Figure 6 illustrates an active heating mode where energy is received from the ambient air and transferred to the chiller bypassing the cabin cooler by a “cold” coolant loop. The heat is then “pumped” by a vapor compression cycle with some heat addition by the compressor to the “hot” loop condenser, where it is transferred into the “hot” loop coolant and later released into the cabin by a coolant-to-air heater.

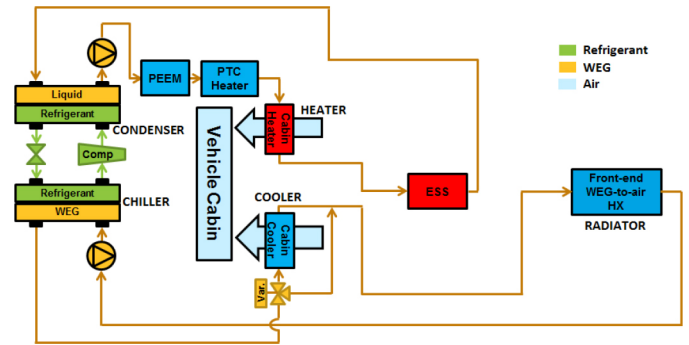


Figure 6. Active heating mode using a heat pump

With the new coolant loop solution method, no identification of coolant loops by the user is needed. The selection of operating modes is done in a more natural way by opening and closing the valves presented in Figure 4. This is different from the previous approach presented in [8], where Figures 2 and 3 illustrated user-specified coolant loops. In this regard, the new approach is a significant improvement in usability of the CoolSim framework for complex systems.

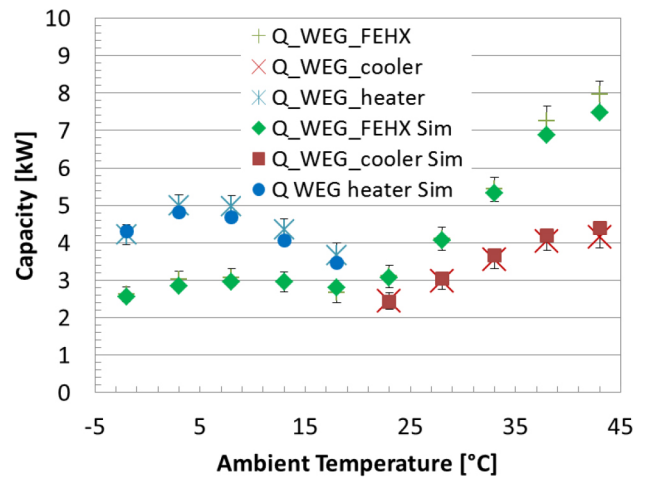


Figure 7. Simulated and measured capacities of coolant-to-air heat exchangers (HX). RMS=4.18%. Nine out of 10 points fall within 95% of uncertainty intervals. Error bars show 95% confidence intervals for measurement uncertainties.

Figures 7 through 10 show steady-state results obtained with the updated coolant loop solution method for the active heating and active cooling modes of the CFL system illustrated in Figures 5 and 6. Data from NREL's experimental test bench span ambient temperature range from -2°C to +43°C. A total of five points were below an ambient temperature of 20°C, for which the active heating mode was used. The remaining five points were above 20°C, for

which the active cooling mode was engaged. Simulation results are compared to the measured data as plots of major parameters versus ambient temperature.

The predicted and measured radiator, heater, and cooler capacities are compared in Figure 7. Figure 8 illustrates a comparison for the condenser and the chiller capacities. The root mean square (RMS) difference between the simulation results and data characterizing the simulation error for capacities of coolant-to-air heat exchangers is 4.18%.

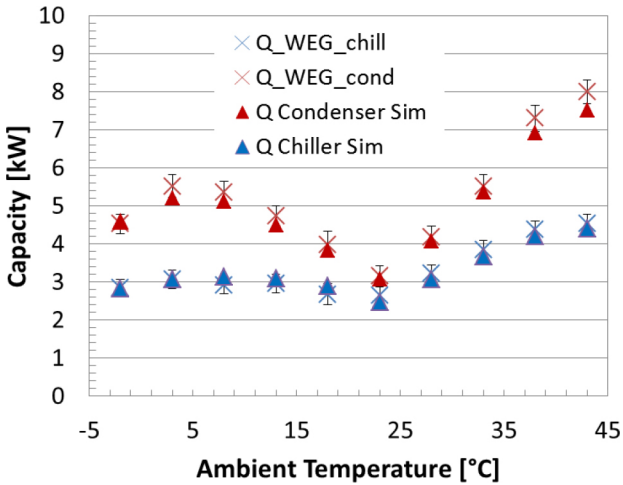


Figure 8. Simulated and measured capacities of coolant-to-refrigerant heat exchangers RMS=4.18%. Error bars show 95% confidence intervals for measurement uncertainties.

In Figure 9, simulated coolant temperatures are compared to the data in each of the five heat exchangers of the system. Figure 10 shows a comparison between the simulated and measured compressor suction and discharge refrigerant pressures. The RMS for the coolant temperatures was found to be 1.56%, for refrigerant pressures 6.71%, and for heat transfer rates 4.18%.

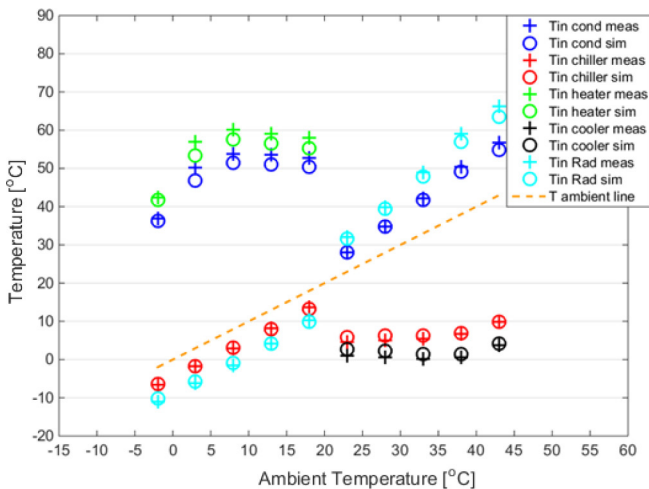


Figure 9. Simulated and measured coolant temperatures in heat exchangers. RMS=1.56%

Figures 7 through 10 together give a quantitative view into the system behavior as well as illustrating the level of accuracy obtained by the new simulation method, which is found to be acceptable and within the error levels of the test data.

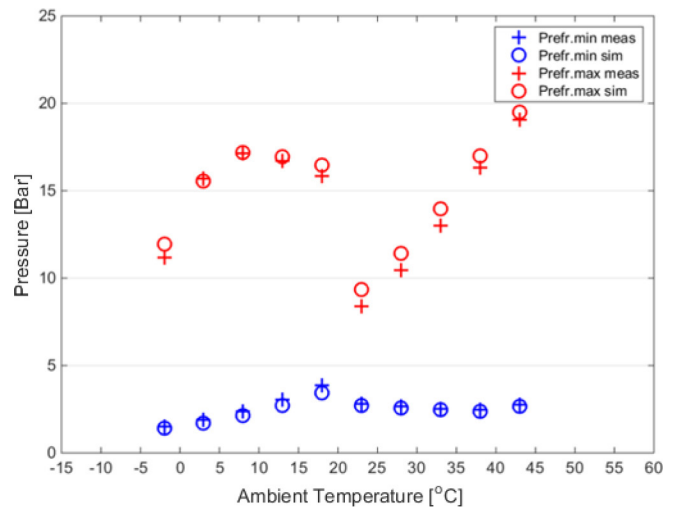


Figure 10. Simulated and measured maximum and minimum refrigerant pressures in the vapor compression circuit. RMS=6.71%

Summary/Conclusions

NREL's MATLAB/Simulink thermal modeling framework, CoolSim, was improved with an alternative simulation method for liquid coolant networks. The new method makes it possible to apply CoolSim to networks with changing flow patterns and flow directions regardless of complexity. This allows the use of a single model whose top-level representation in MATLAB/Simulink closely follows the system schematics for all modes of operation. Such a capability is of special interest to emerging combined refrigerant/coolant loop networks of advanced electric and hybrid vehicles, which may include multiple operating modes. Developing control algorithms for such networks can be greatly simplified by application of CoolSim. Several projects that utilize this capability are now underway with industry partners.

The new simulation method also reduces user effort needed to create more complex system models by eliminating the time-consuming identification of coolant loops that was necessary for the previous "Fluid Network" modeling method. The new method makes it much easier to simulate all of the operating modes in systems with a large number of possible operating modes due to complex configuration and a multitude of on/off valves.

The new approach was validated with the data obtained by NREL's combined loop experimental test bench and showed the same level of agreement with data as the original approach as reported in [12]. The RMS differences between data and simulation for coolant loop parameters were on the order of 5%. These results are overall within uncertainties of the measurements and constitute an acceptable level of agreement with data.

References

1. Rugh, J., Hovland, V., Andersen, S.O., 2004. Significant fuel savings and emission reductions by improving vehicle air conditioners. In: 15th Annual Earth Technologies Forum and Mobile Air Conditioning Summit, Washington, US.

2. Francfort, J., and Murphy, T., "Operational and Fleet Testing, A. Hybrid Electric Vehicle Testing." Chapter V. Advanced Vehicle Technology Analysis and Evaluation Activities: FY 2007 Annual Report. Washington, D.C.: Vehicle Technologies Program, U.S. Department of Energy, 2007; p. 145.
3. Umezu et al., 2010. SAE Automotive Refrigerant and System Efficiency Symposium.
4. Rask, E., et al. 2014. "Ford Focus BEV In-depth (Level 2) Testing and Analysis." Presentation. DOE Annual Merit Review.
5. "Autonomie." www.autonomie.org.
6. Kiss, T., Chaney, L., and Meyer, J., "A New Automotive Air Conditioning System Simulation Tool Developed in MATLAB/Simulink," *SAE Int. J. Passeng. Cars - Mech. Syst.* 6(2):826-840, 2013, doi:[10.4271/2013-01-0850](https://doi.org/10.4271/2013-01-0850).
7. Kiss, T. and Lustbader, J., "Comparison of the Accuracy and Speed of Transient Mobile A/C System Simulation Models," *SAE Int. J. Passeng. Cars - Mech. Syst.* 7(2):739-754, 2014, doi:[10.4271/2014-01-0669](https://doi.org/10.4271/2014-01-0669).
8. Kiss, T., Lustbader, J., and Leighton, D., "Modeling of an Electric Vehicle Thermal Management System in MATLAB/Simulink," SAE Technical Paper 2015-01-1708, 2015, doi:[10.4271/2015-01-1708](https://doi.org/10.4271/2015-01-1708).
9. Streeter, V.L., and Wylie, E.B., *Fluid Mechanics*. 7th edition, McGraw-Hill, New York, ISBN 0-07-062232-9, 1979.
10. Incropera, F.P., and DeWitt, D.P., 2011. *Fundamentals of Heat and Mass Transfer*. 2nd edition, John Wiley and Sons: New York, NY.
11. Chang, Y., and Wang, C., "A Generalized Heat Transfer Correlation for Louver Fin Geometry," *Int. J. Heat Mass Transfer* 40(3):533-544, 1997.
12. Leighton, D., and Rugh, J., 2014. "Electric Drive Vehicle Range Improvement Using a Combined Fluid Loop Thermal Management Strategy." Presentation at the SAE Thermal Management Systems Symposium, Sept. 22-24, 2014, Denver, CO.

Acknowledgments

The authors would like to thank David Anderson and Lee Slezak, Technology Managers for the U.S. Department of Energy's Advanced Vehicle Technology Analysis and Evaluation for sponsoring this work.

MAHLE Inc. is acknowledged for component data and useful discussions.

Thank you to Lisa Fedorka of NREL for providing administrative support for the paper.

This work was supported by the U.S. Department of Energy under Contract No. DE-AC36-08GO28308 with the National Renewable Energy Laboratory. Funding provided by U.S. DOE Office of Energy Efficiency and Renewable Energy Vehicle Technologies Office.

The U.S. Government retains and the publisher, by accepting the article for publication, acknowledges that the U.S. Government retains a nonexclusive, paid-up, irrevocable, worldwide license to publish or reproduce the published form of this work, or allow others to do so, for U.S. Government purposes.

Definitions/Abbreviations

A/C - air conditioning

CFL - combined fluid loop

EV - Electric vehicle

NREL - National Renewable Energy Laboratory

RMS - root mean square

WEG - water-ethylene glycol

Contact Information

Eugene Titov
eugene.titov@nrel.gov

Jason Lustbader
jason.lustbader@nrel.gov

The Engineering Meetings Board has approved this paper for publication. It has successfully completed SAE's peer review process under the supervision of the session organizer. The process requires a minimum of three (3) reviews by industry experts.

All rights reserved. No part of this publication may be reproduced, stored in a retrieval system, or transmitted, in any form or by any means, electronic, mechanical, photocopying, recording, or otherwise, without the prior written permission of SAE International.

Positions and opinions advanced in this paper are those of the author(s) and not necessarily those of SAE International. The author is solely responsible for the content of the paper.

ISSN 0148-7191

<http://papers.sae.org/2016-01-0230>